



Published in final edited form as:

Acta Biomater. 2017 January 1; 47: 71–80. doi:10.1016/j.actbio.2016.09.045.

Overcoming Cisplatin Resistance in Non-Small Cell Lung Cancer with *Mad2* Silencing siRNA Delivered Systemically using EGFR-Targeted Chitosan Nanoparticles

Ana Vanessa Nascimento^{a,b,c,d}, Amit Singh^c, Hassan Bousbaa^{a,e}, Domingos Ferreira^b, Bruno Sarmiento^{a,d}, and Mansoor M. Amiji^{c,*}

^aCESPU, Instituto de Investigação e Formação Avançada em Ciências e Tecnologias da Saúde, Gandra, Portugal

^bLaboratory of Pharmaceutical Technology, Faculty of Pharmacy, University of Porto, Portugal

^cDepartment of Pharmaceutical Sciences, School of Pharmacy, Bouvé College of Health Sciences, Northeastern University, Boston, USA

^dI3S, Instituto de Investigação e Inovação em Saúde and INEB—Instituto de Engenharia Biomédica, Universidade do Porto, Portugal

^eCentro Interdisciplinar de Investigação Marinha e Ambiental (CIIMAR/CIMAR), Universidade do Porto, Portugal

Abstract

Efficiency of chemotherapy is often limited by low therapeutic index of the drug as well as emergence of inherent and acquired drug resistance in cancer cells. As a common strategy to overcome drug resistance, higher doses of chemo-agents are administered. However, adverse side effects are usually increased as a consequence. A potentially effective approach is to combine chemotherapy with other therapeutic strategies such as small interfering RNAs (siRNAs) that allow the use of lower yet efficient doses of the anticancer drugs. We previously developed epidermal growth factor receptor (EGFR)-targeted chitosan (CS) nanoparticles as a versatile delivery system for silencing the essential mitotic checkpoint gene *Mad2*, and induce cell death. Here, we tested this system as a single therapy and in combination with cisplatin in cisplatin sensitive and resistant lung cancer models, and characterized its *in vivo* efficacy and safety. Combination treatment resulted in significant improvement in tumor inhibition that was strikingly more effective in cisplatin-resistant tumors. Importantly, effective cisplatin dosage was dramatically reduced in the co-therapy regimen resulting in negligible toxic effects from the drug

*Corresponding Author. Tel.: (617) 373-3137. Fax: 617-373-8886. m.amiji@neu.edu.

Publisher's Disclaimer: This is a PDF file of an unedited manuscript that has been accepted for publication. As a service to our customers we are providing this early version of the manuscript. The manuscript will undergo copyediting, typesetting, and review of the resulting proof before it is published in its final citable form. Please note that during the production process errors may be discovered which could affect the content, and all legal disclaimers that apply to the journal pertain.

Conflict of Interest

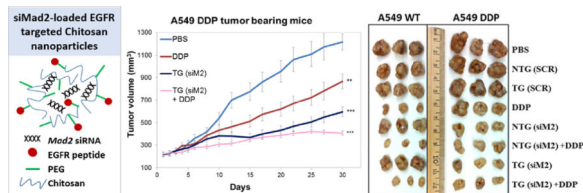
No potential conflicts of interest were disclosed.

Supporting Information Available

Experimental treatment groups, dose regime schemes and *in vitro* *Mad2* expression in the A549 WT and A549 DDP cell line after dosing with si*Mad2*-loaded NTG and TG CS nanoparticles.

as confirmed by parameters such as body weight gain, biochemical markers of hepatic and renal function, and histopathology of liver/kidney/spleen tissues. Overall, we demonstrate that the combination of Mad2 siRNA-loaded CS nanoparticles strategy with chemotherapeutic agents such as cisplatin constitutes an efficient and safe approach for the treatment of drug resistant tumors.

Graphical Abstract



Keywords

Cisplatin resistance; EGFR-targeted chitosan nanoparticles; Mad2 siRNA delivery; non-small cell lung cancer models; efficacy; safety profile

1. Introduction

Lung cancer is the leading cause of cancer related death in both men and women in the United States [1]. Non-small cell lung cancer (NSCLC) represents 87% of the cases of lung cancer [2]. Most of NSCLC patients are frequently diagnosed with advanced-stage disease and have a 5-year survival rate of only 17.4%, lower than many other cancer sites [1, 2]. Cisplatin (cis-diamminedichloroplatinum (II)) (DDP) is usually the first-line chemotherapeutic treatment in combination with other drugs such as gemcitabine, vinorelbine, docetaxel, or paclitaxel [3, 4]. Uptake of cisplatin in the cells is facilitated by copper transporters and upon entry, the drug is hydrolyzed to form a potent electrophile that binds and reacts to nucleophiles such as sulfhydryl group of proteins and N7 reactive centers of purine residues of DNA to form adducts. This leads to cessation of cell division and rapid cell death due to oxidative stress, DNA damage and activation of the apoptotic machinery of the cell [5]. Cisplatin cytotoxicity primarily stems on its ability to interact with DNA, forming platinum-DNA adducts that inhibit DNA replication. Cell cycle checkpoints monitor the accurate order of events during cell division, including DNA damage and when an error is detected, a delay occurs to provide time for damage repair [6, 7]. Cisplatin causes arrest during cell cycle G2/M phase in cells with an intact DNA damage checkpoint [8]. In case cells are not able to repair DNA damage, two different modes of cell death are induced, necrosis and apoptosis [9]. If G2/M phase arrest fails, the cell will continue the cycle and on the mitotic phase (M phase), the spindle assembly checkpoint (SAC) can be activated and either initiate DNA repair, or initiate apoptosis [10]. Cisplatin therapy has two major complications - the augmentation of tumor therapeutic resistance and significant systemic off-target effects [5]. In terms of mechanisms responsible for the acquired resistance to cisplatin, several factors have been identified that include decreased cytoplasmic accumulation; cytoplasmic sequestration; enhanced DNA repair [11, 12]. Tumor resistance could be circumvented by the use of higher doses but that would aggravate the secondary

effects (nephrotoxicity, emetogenesis and neurotoxicity), mostly due to non-specificity of drug [13]. Novel approaches are therefore needed to circumvent these therapeutic challenges.

The demand of new strategies, the constant improved knowledge of cancer molecular biology and nanotechnology innovation in the last few decades has made gene therapy a novel and attractive treatment modality [14, 15]. The addition of gene therapy could significantly augment cancer drugs efficacy and allow lower doses, alleviating their secondary effects. On the other hand, although gene therapies are more specific, they are not as potent and widespread as chemotherapeutic agents. Gene therapy also benefits and its efficacy is significantly augmented when used together with chemotherapy [15]. Chemotherapy and gene therapy is therefore a promising combination strategy for the treatment of aggressive tumors such as lung cancer.

Strategies targeting mitosis in cancer has been an established clinical approach not only with classical microtubule-targeting drugs but also with newly proposed small molecules targeting Aurora kinases, kinesin spindle proteins, Polo-like kinases, etc [16, 17]. Mitotic arrest deficient-2 (Mad2) is an essential component of the mitotic checkpoint that has a crucial role in the correct segregation of chromosomes during mitosis [18]. Mad2, together with other checkpoint proteins, delays anaphase until all chromosomes are attached to the mitotic spindle, assuring the fidelity of chromosome segregation in mitosis [7].

Mad2 is involved both in the SAC and in G2/M phase checkpoint although its role in the DNA damage response was only recently described and is still unclear [19]. It is suggested that Mad2 is involved in the DNA damage response pathway leading to mitotic arrest and activation of apoptosis pathway [19, 20]. The dual implication of Mad2 on both surveillance mechanisms, SAC and G2/M phase checkpoints can explain previous findings that showed that Mad2 overexpression conferred sensitivity to DNA-damaging agents, especially cisplatin, associated with induction of cell cycle arrest [21].

The opposite effect can also be used as a therapeutic strategy. Mad2 knockdown leads to an early mitosis exit, increased level of severe segregation errors and extensive cell death [22–24]. This process is designated by mitotic catastrophe and although a small minority of daughter cells could survive, they are condemned to death due to the absence of genes coding for essential proteins [25]. On the other hand, since Mad2 is a mitotic protein, its gene silencing will mainly affect cells with increased cell division, one of the hallmarks of tumor cells [26]. The selectivity and the severe impact of Mad2 silencing on cancer cells, makes this approach a very attractive alternative therapy.

Mad2 silencing is a compelling method that can be achieved by RNA interference (RNAi)-based therapeutics. RNAi has the potential to become a powerful therapeutic approach in many illnesses such as cancer since it allows to specifically target gene sequences involved in the mechanism of proliferation, apoptosis evasion, drug resistance, and metastasis [27]. The major challenge in RNA-based therapeutics *in vivo* is to ensure tumoral delivery of siRNAs [28]. Unprotected siRNA present a short half-life due to serum nuclease degradation and renal clearance, and are not easily taken up by the cells [28]. These difficulties could be

overcome by carefully choosing a suitable delivery vector with characteristics such as biocompatibility, biodegradability and non-immunogenicity [29]. Chitosan (CS) is a nonviral vectors extensively used for nucleic acid delivery *in vitro* and *in vivo* because of its mucosa permeation properties, high biocompatibility, low toxicity and biodegradability [30]. This natural polysaccharide is composed of glucosamine and *N*-acetylglucosamine residues resulting from partial deacetylation of chitin [31]. CS is available with different degree of deacetylation, molecular weight and depending on the pH, the deacetylated amine groups along the CS chain will be protonated and available to interact with the negatively charged siRNA [31]. CS is capable of protecting siRNA, increasing its stability in the blood stream but also, the innumerable chemical modification that can be done to its structure, make it capable of enhancing cell specificity and transfection efficiency [32]. The addition of different groups to CS backbone allows to functional moieties to be added, like cell-targeted ligands, making CS an efficient and versatile drug delivery platforms [33, 34]. One common modification is the anchoring of poly(ethylene glycol) (PEG) chains to the nanoparticle surface which is used to improve the circulatory half-lives of therapeutics and higher tumor accumulation [35]. This effect is associated to the enhanced permeability and retention (EPR) effect that describes the preferential accumulation of nanoparticles at tumor sites due to leaky vasculature [35]

In our previous *in vitro* study, we successfully developed an epidermal growth factor receptor (EGFR)-targeted chitosan system capable of silencing *Mad2* gene and inducing cell death in EGFR overexpressing human A549 cell line [23]. Here, we have investigated the effects of siRNA targeting *Mad2* (siMad2) alone or in combination with cisplatin at sub-therapeutic dosage. This study was performed in mice bearing subcutaneous, cisplatin sensitive or resistant, human lung adenocarcinoma xenograft tumors, with the aim of examining its efficacy in the inhibition of tumor growth.

2. Materials and Methods

2.1 Materials

The following products were purchased from Sigma-Aldrich Inc. (St. Louis, MO): ALT Activity Assay Kit (CAT. MAK052); AST Activity Assay Kit (CAT. MAK055); Blood Urea Nitrogen Assay Kit (CAT. MAK006); Creatinine Assay Kit (CAT. MAK080); CS (MW = 55kDa; degree of deacetylation of 75–85%); cisplatin (CAT. P4394). A pool of 3 sequences of siRNA duplexes targeted against *Mad2* mRNA (CAT. sc-35837) and a non-targeting negative control duplexes (CAT. sc-37007) were purchased from Santa Cruz Biotechnology Inc. (Dallas, TX). All primers were customized and ordered from Eurofins Scientific (Luxembourg City, Luxembourg). EGFR-specific peptide was synthesized at Tufts University's Peptide Synthesis Core Facility (Boston, MA). Succinimidyl-([N-maleimidopropionamido]-ethyleneglycol) ester (MAL-PEG₂₀₀₀-NHS, MW 2,000 Da) was purchased from JenKem (Allen, TX). All cell culture material was purchased from Invitrogen/Life Technologies (Carlsbad, CA). The BMP LeukoChek Test Kit to count white blood cells (WBC) and platelets was acquired from Biomedical Polymers, Inc. (Gardner, MA).

2.2 Cell lines

A549 human lung adenocarcinoma cells were obtained from American Type Culture Collections (Manassas, VA). A cisplatin-resistant version of this cell line (A549-DDP) was obtained from Massachusetts General Hospital (Boston, MA). Both cell lines were cultured in DMEM/F12 medium from Life Technologies (Carlsbad, CA) supplemented with 10% FBS and penicillin/streptomycin (100 U/mL) (Thermo Fisher Scientific, Waltham, MA, USA) and grown at 37°C, 5% CO₂. A549-DDP cells were cultured with 2 µg/mL (6.7 µM) cisplatin to maintain their drug-resistant phenotype. The resistant phenotype of these cells was regularly assessed by cytotoxicity analysis to ensure their IC₅₀ (dose that kills 50% of cells) values.

2.3 Synthesis and Characterization of Control and Epidermal Growth Factor Receptor-Targeted Chitosan Derivatives

PEGylated CS and EGFR-targeted CS derivatives were synthesized according to our previously optimized and established protocol reported elsewhere [23, 33]. Briefly, a 10% molar equivalent of Mal-PEG₂₀₀₀-NHS was added to a 2 mg/mL CS solution in 2% acetic acid and left to react overnight at room temperature. The product was purified by dialysis (10 kDa cutoff) and reacted with either cysteine or EGFR targeting peptide (i.e., YHWYGYTPQWVI-*GGGG-C*) to obtain PEG-modified (non-targeted control) and EGFR-targeted CS respectively. Proton nuclear magnetic resonance (¹H-NMR) spectroscopy was employed to characterize both derivatives. All NMR samples were prepared by dissolving 2–4 mg of the lyophilized product in 0.7 mL of D₂O with 0.2% DCl and characterized by 400 MHz ¹H NMR spectroscopy (Varian, Inc. CA).

2.4 Nanoparticle Formulation and Characterization

A pool of 3 sequences of siRNA duplexes targeted against the Mad2 mRNA was encapsulated in CS nanoparticles by self-assembly in aqueous solution maintaining a N/P ratio of 50 [23, 33]. The non-targeted (NTG) nanoparticles were obtained by encapsulating siMad2 in PEGylated CS. The targeted (TG) nanoparticles were achieved with a 50 % (w/w) mixture of PEGylated CS and EGFR-targeted CS to encapsulate siMad2. The average hydrodynamic diameter and the polydispersity index (PDI) of the nanoparticles were measured by dynamic light scattering at room temperature and a 90° fixed angle using Zetasizer ZS (Malvern, Worcestershire, UK) [23]. Similarly, the zeta potential of the nanoparticles was measured using an electrophoretic cell. The siRNA encapsulation efficiency in the nanoparticle formulation was calculated by the formula: encapsulation efficiency (%) = ((total amount of siRNA – free siRNA)/(total amount of siRNA)) × 100. Loading capacity was determined by the formula: loading capacity (%) = (weight of loaded siRNA/weight of polymer) × 100. For every study, nanoparticles were freshly prepared and dissolved in PBS in order to obtain a desired concentration and also achieve an osmolarity of 300 mOsm/kg and a pH of 7.2.

2.5 In Vitro Cytotoxicity Studies for Cisplatin in Combination with siRNA Therapy

A549 WT and A549-DDP cells were cultured overnight at a cell density of 3000 cells/well in a 96-well plate in 200 µl of supplemented culture media. The cells were washed and 100

μL of the nanoparticle solution was added to each well ($n=8$), incubated at 37°C for 6 h, and followed by replacement of the solution with complete growth medium. After a 48 h, growth media was replaced with serum-supplemented media containing $0.01\ \mu\text{M}$ – $10,000\ \mu\text{M}$ cisplatin as free drug. Cell toxicity was assessed 24 h later by the MTT (3-(4,5-dimethylthiazol-2-yl)-2,5-diphenyltetrazolium bromide) assay. For that, medium was replaced with fresh complete medium containing $100\ \mu\text{L}$ of $0.5\ \text{mg/mL}$ MTT (Sigma-Aldrich, St. Louis, MO) for two hours. Then, medium was replaced by dimethyl sulfoxide (DMSO) to stop the reaction and lyse the cells. Absorbance of the solution was measured at $560\ \text{nm}$, and the IC_{50} was calculated using GraphPad Prism software. Untreated cells served as a negative control and cells incubated with poly(ethyleneimine) (PEI, MW 10kDa), a known cytotoxic cationic polymer, were used as positive control for all cytotoxicity experiments.

2.6 Human Lung Adenocarcinoma Xenograft Tumors

Animal procedures were performed according to a protocol approved by Northeastern University, Institutional Animal Care and Use Committee (NUIACUC). Five to six weeks old female *nu/nu* (athymic) mice, strain CrTac:NCr-Foxn1nu, weighing approximately 20 g, were purchased from Taconic Biosciences, Inc. (Hudson, NY). The animals were allowed to acclimate for at least 72 h prior to any experimentation, raised under specific pathogen-free conditions, kept in individually ventilated cage racks and supplied with sterile rodent pellets and water *ad libitum*. Mice were housed under a 12 h light/dark cycle.

For A549-WT and A549-DDP tumor model development, mice were injected subcutaneously with 3×10^6 cells in a mixture of $50\ \mu\text{L}$ DMEM/F12 medium and $50\ \mu\text{L}$ Matrigel under mild anesthesia on their right flank. Tumor volume was calculated by the modified ellipsoid formula: tumor volume = $1/2(\text{length} \times \text{width}^2)$. When tumors grew to approximately $200 \pm 20\ \text{mm}^3$ in volume the animals were randomized into groups to yield even distribution of tumor sizes. Sample size was determined by power analysis using the software G*Power. Each animal was identified with an ear tag which allowed us to perform blind experiments in order to reduce bias in animal selection and outcome assessment. The animals were monitored daily for food/water intake, body weight and any physical signs of discomfort.

2.7 In Vivo Mad2 Gene Knockdown in A549 WT and A549-DDP Tumor Models

A single dose of $3\ \text{mg/kg}$ of encapsulated siRNA was intravenously injected into A549-WT or A549-DDP tumor model accordingly to different treatment groups (Supporting Information (SI)1) and at different time points, tumors were collected for RNA and protein extraction.

The tumors were homogenized in RNALater solution and tissue total RNA was extracted using GeneJET RNA Purification Kit from Thermo Fisher (Waltham, MA). For cDNA synthesis, $0.5\ \mu\text{g}$ of total RNA was used with Verso cDNA synthesis kit (Thermo Fisher Scientific, Waltham, MA) according to the manufacturer's instructions. Mad2 siRNA was quantified by qPCR with LightCycler 480 SYBR Green I Master kit (Roche, Basel, Switzerland) and primers for 28S ribosomal gene as endogenous control. The sequences of

the primers used were: Mad2-fw (GTGGAACAACCTGAAAGATTGGT), Mad2-rv (GTCACACTCAATATCAAACCTGC), 28S-fw (GGGTTTAGACCGTCGTGAGA), 28S-rv (TCCTCAGCCAAGCACATACA). Mad2 gene expression levels were normalized against 28S ribosomal expression levels, which has shown to have a stable expression throughout the tissues.

For Western blot analysis, tumors were homogenized in lysis buffer for protein extraction. The BCA Protein Assay Kit was utilized to measure the protein concentration. Protein were separated on 4–20% gradient SDS-PAGE gels and transferred onto a PVDF membrane. The membrane was blocked incubating it for 2 h in blocking buffer (Abcam). The membrane was incubated with primary antibody overnight at 4° C, washed with TBST and later incubated with HRP secondary antibody for 2 h. The bands were visualized after incubation with chemiluminescence detection reagent (Pierce) as described in the manufacturer's instructions. The primary antibodies used were the rabbit anti-Mad2 (1:500; Abcam, #ab180579) and the mouse anti-tubulin (1:5000; Abcam, #ab80779); the secondary were goat anti-rabbit HRP (horseradish peroxidase) secondary antibody (1:5000; SantaCruz, #SC-2054) and goat anti-mouse HRP secondary antibody (1:5000; SantaCruz, #SC-2005). Tubulin was used as a protein loading control.

2.8 In Vivo Efficacy Studies for the Combination Treatment of Mad2 siRNA/Chitosan Nanoparticles and Cisplatin Solution

Animals bearing A549 WT or A549-DDP tumors with a volume close to $200 \pm 20 \text{ mm}^3$ were randomized into 8 groups (n=8). At day 1, siMad2 (3mg/kg dose) encapsulated in NTG or TG nanoparticles was administered intravenously via tail vein and 48 h later (day 3), cisplatin (1 mg/kg dose) in solution was administered intravenously (SI 2A). This 5-day dosage regimen was repeated 6 times over the course of 30 days of therapy. As a negative control, one group was administered with saline solution (SI 2B). One group of animals was injected only with cisplatin (1 mg/kg) and 2 set of groups were given NTG or TG nanoparticles with scrambled sequence (SCR). Tumor volume was measured daily for the first week and every 2 days for the rest of the study. At day 30, animals were sacrificed by isoflurane inhalation followed by cervical dislocation. Blood was collected from all groups in order to assess safety parameters. Liver, kidney, and spleen samples from mice were also collected for histopathological analysis.

2.9 Measuring Body Weight Changes, Liver and Kidney Enzyme Levels Quantification, White Blood Cells Count and Platelets

Mice of different experimental groups were weighed daily until the end of the first week and every two days until the end of the experiment. The body weight change was calculated and recorded as mean \pm standard deviation (SD). Blood was collected in EDTA coated K2 tubes (Greiner Bio-one, Monroe, NC) from all groups at the end of the study and different parameters were measured. Alanine aminotransferase (ALT) and aspartate aminotransferase (AST) levels were assessed as indicator of liver damage and serum creatinine and blood urea nitrogen as indicators of kidney function. WBC and platelets were also counted. All these parameters were measured using the kits mentioned in the materials section and used accordingly to the manufacturer's instructions.

2.10 Tissue Histopathological Analysis

Liver, kidney, spleen and tumor samples from mice were collected for histopathological analysis at the end of the efficacy study. The tissue samples were processed for histological sectioning, H&E staining, and analysis at the Veterinary Clinical Laboratory INNO (Braga, Portugal).

2.11 Statistical Analysis

Comparisons between two groups were made using Student's T-test and with more than two groups, the ANOVA test was used. A value of $p < 0.05$ was considered to be statistically significant. Data is presented as means \pm standard deviation.

3. Results and Discussion

Targeted nanosystems have come a long way in developing clinically safe and efficient nanomedicines for delivery of labile therapeutic molecules such as siRNAs [36]. In our previous in vitro study, the EGFR-targeted CS nanoparticles demonstrated a very efficient and targeted delivery of the encapsulated Mad2 siRNA in the A549-WT and A549-DDP cells resulting in silencing the expression of *Mad2* gene [23]. The pharmacokinetics and biodistribution of these nanoparticles in A549-WT and A549-DDP tumor-bearing mice also demonstrate a higher targeting efficiency and accumulation of the EGFR-peptide modified nanoparticles in comparison to non-targeted nanoparticles [37]. The study confirmed that the presence of the EGFR-targeting peptide leads to a higher tumor exposure and therefore can have tremendous therapeutic potential. The present study is aimed to evaluate the therapeutic effect of Mad2 siRNA loaded in CS nanoparticles in A549-WT and A549-DDP tumor bearing mice as single therapy or in combination with cisplatin. As previously described, NTG and TG nanoparticles used in this study were in the size range of 100–230 nm, surface charge ranging between +28 to +35 and high encapsulation efficiencies (Table 1) [23]. These nanoparticles show a high polydispersity index (PDI), which is consistent with natural polymers such as chitosan primarily since they have a higher degree of variation in chain length. We have always observed and reported a high PDI for these nanoparticles in all our previous work [[23, 33, 37]] and the same has been reported in literature as well [38, 39].

3.1 Mad2 knockdown potentiates cisplatin effects and sensitizes Cisplatin-Resistant Lung Cancer Cells in vitro

Cancer drugs that includes platinum-based compounds such as cisplatin act against cancer cell proliferation by damaging their DNA. As a consequence of this DNA damage, DNA replication is prevented before cell division, which usually induces apoptosis. However, cancer cells can escape apoptosis through translesion synthesis (TLS), a type of DNA replication that is highly prone to errors and, thus, favors drug resistance and tumor aggressiveness [40, 41]. DNA damage in mitosis activates the spindle assembly checkpoint (SAC) which causes cell death after a sustained mitotic arrest [42]. However, because most cancer cells exhibit a weakly functional SAC, they escape mitosis and survive. Complete abrogation of SAC leads to premature cell division with massive chromosome segregation errors that are incompatible with life. We thus reasoned that the suppression of the SAC

component Mad2 by specific siRNA-loaded nanoparticles would kill cancer cells that escape cisplatin effect and, consequently, sensitize cancer cells to chemotherapy.

Our previous efforts towards optimization of CS-siRNA formulation using different weight combination of mixture of EGFR-targeted CS and PEG modified CD showed that a 50% (w/w) mixture gave optimal siRNA activity *in vitro* [23] and therefore this blend was chosen for all subsequent *in vitro* and *in vivo* work. We subsequently characterized the chemical properties of the CS derivatives by nuclear magnetic resonance, physical properties of the nanoparticles using dynamic light scattering and electron microscopy and their targeting nature using a series of control experiments [23]. Based on the prior knowledge, we prepared CS-siRNA formulations using the pre-established protocol and first conducted nanoparticles-mediated gene silencing *in vitro*. We could efficiently achieve the down-regulation of Mad2 expression by NTG and TG nanoparticles in A549-WT and A549-DDP cells, with negligible effect in untreated or blank nanoparticles-treated controls (SI 2 and 3) [23]. We first assessed the 50% inhibitory concentration (IC₅₀) of cisplatin drug in A549-WT and A549-DDP cell lines to ascertain the drug resistance property of the latter. The IC₅₀ of cisplatin was more than tenfold higher in A549-DDP (IC₅₀=140.73 μ M) than in A549-WT (IC₅₀=12.24 μ M), confirming the drug-resistant phenotype of A549-DDP cells (Table 2).

For the combination study, cells were first incubated for 48 h with siMad2-loaded CS nanoparticles containing 50 nM siRNA and later for 24 h with cisplatin at increasing concentrations to determine the drug's IC₅₀. Combination of Mad2 depletion and cisplatin treatment leads to a dramatic increase in cytotoxicity in both cell lines compared to individual treatments, with an even stronger effect in the cisplatin-resistant line. Indeed, a significant decrease in cisplatin IC₅₀, up to 95-fold in the sensitive cell line and to 2495-fold in the resistant cell line, was observed when combined with TG nanoparticles (Table 2). Importantly, in the drug resistant cell line, a strong reduction in cisplatin IC₅₀ (up to 1513-fold) was still achieved even with reduced amount (50-fold lesser) of Mad2 siRNA. Interestingly, gene expression analysis by qPCR revealed that Mad2 mRNA levels was three times less abundant in A549-DDP compared to A549-WT (SI 3A), which may explain why the resistant cell line require a lesser dose of Mad2 siRNA to obliterate the *Mad2* gene activity.

Overall, these results suggest that siRNA-mediated Mad2 downregulation enhances the sensitivity of lung cancer cells to cisplatin with a high level of reversal of drug resistance. The improvement observed in the *in vitro* cytotoxicity profile of TG nanoparticles compared to the NTG nanoparticles seems mainly due to the EGFR peptide modification triggering receptor-mediated endocytosis and this phenomenon has been extensively study in our previous work [23].

Cisplatin, as a crosslinking agent, binds to DNA to form intrastrand and interstrand crosslinks and adducts which initiates changes in DNA conformation and interferes with DNA replication [40, 41]. This culminates in G2/M cell cycle arrest that can lead to DNA repair, promoting resistance to the drug, or resulting in apoptosis [41]. If cells are able to escape G2/M arrest and progress to the mitotic phase, cell will fail to arrest and an aberrant

chromosome segregation will take place in the absence of Mad2, triggering cell death [16, 22]. Due to these underlying mechanisms, the combination of CS nanoparticle containing siMad2 with cisplatin treatment was found to be more effective when compared with cisplatin alone treatment.

3.2 In Vivo Mad2 Gene Silencing in Tumor Bearing Mice

The *in vivo* tumor targeting and gene silencing activity of the TG and NTG nanoparticles was studied in subcutaneous xenograft murine model of A549-WT and A549-DDP cells. Mad2 silencing was analyzed both at mRNA and protein levels in tumor extracts harvested from the mice at the designated time points. As shown in figure 1A, Mad2 mRNA levels decreased to 20% of the control at 48 h post-treatment in both sensitive and resistant tumor models with TG nanoparticles being more efficient than NTG nanoparticles. A similar response was also observed in Mad2 protein level, which was reduced to 35% of the control in A549-WT and 22% in A549-DDP (Figure 1B). Interestingly, the silencing effect of a single dose of nanoparticles persisted for as long as 96 h post-treatment, demonstrating the effectiveness of the nanoparticles in inhibiting Mad2 expression in tumors. Besides, for all the time points assessed, the silencing effect was more pronounced in the drug resistant cells when compared to their sensitive counterparts. Importantly, such prolonged knockdown of the Mad2 gene would aid in providing a synergy of combination treatment with cisplatin.

3.3 In Vivo Therapeutic Efficacy Assessment of siMad2/Cisplatin Combination

Once the *in vivo* activity of Mad2 siRNA was confirmed, the next aim was to determine whether treatment with Mad2-siRNA nanoparticles formulations would result in increased sensitivity or even reversal of drug resistance in cells. The tumor bearing mice were administered with 6 doses of combination treatment of Mad2 siRNA and cisplatin as per the dosing schedule and the treatment groups (SI 2A and B). Among all the treatment groups, a combination treatment with Mad2 siRNA encapsulated in TG nanoparticles (dose 3 mg/kg) and cisplatin (dose 1 mg/kg) outperformed all other single or combination therapies in both the tumor models (Figure 2).

None of the controls had any significant effect on tumor growth. Both sensitive and resistant tumors treated with Mad2-siRNA nanoparticles displayed delayed tumor growth, which was more accentuated with TG (A549-WT: 45 %; A549-DDP: 51.2 %) than with NTG nanoparticles (A549-WT: 26.2 %; A549-DDP: 43 %) (Figure 3). As expected, cisplatin as single treatment was more effective in sensitive than in resistant tumors. TG nanoparticles, and to a lesser extent NTG nanoparticles, plus cisplatin resulted in the greatest efficacy in both lung tumor models (NTG (siM2) + DDP: 58.9 %; TG (siM2) + DDP: 70.6 %). These results strongly suggests that the combinational effects of Mad2-siRNA-loaded nanoparticles and an anticancer drug such as cisplatin can be a valuable therapeutic strategy to increase drug sensitivity and overcome resistance.

Interestingly, our biodistribution and pharmacokinetic studies using the NTG and TG nanoparticles in the same tumor models revealed that TG system has tumor exposure than the NTG system and also demonstrate better targeting efficiency [37], we do not see a corresponding increase in efficacy. The *in vitro* data also corroborate that TG nanoparticles

are able to internalize more efficiently than the NTG nanoparticles [23]. It is established that cancerous cells show an obliterated control over mitotic checkpoints due to significant loss of activity of the checkpoint genes. A closer look at the *in vivo* efficacy data set (Figure 2) reveals that the remnant *Mad2* activity is extremely important to the cancerous cells, especially A549-DDP, where the knockdown of the activity led to significant loss in the tumor growth. This is supported by the fact that both NTG and TG nanoparticles performed better than cisplatin group, which is ineffective due to drug resistance. We therefore believe that the dose of the siRNA provided by both the nanoparticles is sufficient to knockdown the *mad2* activity sufficiently to mask the effect of targeting. An *in vivo* study based on different dose of siRNA loaded in the NTG and TG nanoparticles would probably be able to discern the targeting effect.

Tumor vascularity plays a key role in the localization of the nanoparticles and human NSCLC shows poor vascularity. Such tumors with hypoxic necrotic core would be an attractive target for targeted therapy approach such as ours for two reasons; the increased tumor targeting efficiency as confirmed by pharmacokinetic analysis and the increased tumor residence time and activity (up to 96 h) shown by the efficacy studies. However, nanoparticle penetration into the extremely heterogeneous tumor microenvironment with poor vascularity is a significant challenge that has to be overcome. Therefore, efficacy study in a more clinically relevant orthotopic model or patient-derived xenograft would be essential to cement the robustness of our therapeutic approach and assess its translational capability.

3.4 In Vivo Acute Safety Analyses

Safety of any drug is of paramount importance to the well being of the patients and recent trends clearly suggest that a vast majority of the potential preclinical candidates fail during the clinical trials due to adverse safety profile. Therefore we monitored the safety of the formulations closely during the course of therapy as a function of the body weight of animals in each treatment groups (Figure 4A). Initially all the animals showed a slight decrease in body weight which could be due to handling stress but the animals quickly recovered to their initial weight and gained weight during the course of the therapy (Figure 4A).

There was no statistical significance in the average body weights of the animals from different treatment groups suggesting that none of the therapeutic regimen led to any adverse effect of animal body weight.

In addition to the body weight, some serum safety markers were analyzed in order to evaluate the safety of nanoparticle administration to the animals. The PK/PD analysis of these nanoparticles in tumor bearing animals showed a significant concentration of the CS nanoparticles infiltrating into the liver and kidney and therefore a toxic impact to these organs was a major concern [37].

We measured the concentrations of the enzymes AST and ALT as an indicator of any liver health and function; serum creatinine and blood urea nitrogen as an indicator of kidney function and WBC and blood platelets count to ensure. There was no significant elevation in

the liver enzymes levels during the course of the therapy, suggesting that none of the nanoparticle system caused any liver damage (Figure 4B). Similar results were also obtained for the blood creatinine and urea nitrogen indicating a healthy kidney function in all the treatment groups (Figure 4B). Elevated WBC counts is often associated with tissue damage and a decrease in platelet counts are indicative of chemotherapy toxicity. WBC and platelets number were found to be consistent between the different experimental groups (Figure 4B) including control suggesting that the administration of CS nanoparticles to the animals alone or in combination with cisplatin drug did not have any toxic implication to the animals.

At end of the study, the liver, kidney and spleen of mice from each group of both tumor models were collected and tissue sections were used for hematoxylin and eosin staining (Figure 5). For all the groups in both the tumor models, the tissues did not show any pathological changes in the histology analysis, which is in agreement with the serum safety markers analyzed previously. We were not expecting toxicity from cisplatin as well since the administered dose was very low compared to the clinical dose.

4. Conclusions

In summary, EGFR-targeted chitosan nanoparticles were employed as a new delivery carrier for Mad2 siRNA in combination with cisplatin to achieve maximal therapeutic efficacy by overcoming chemo-drug resistance in NCSLC. Both siRNA and cisplatin were used at low but effective doses, minimizing adverse side effects. In this study, we evaluated two formulations that differ in the presence of a target moiety. The targeted delivery showed effective and improved tumor growth inhibition when compared to non-targeted and this effect was even more pronounced when used in combination with cisplatin. Also, Mad2 siRNA results in mitotic failure and extensive cell death but the advantage of such strategy is that it preferentially affects mitotic cells, so highly proliferative tumors will be the most affected. Collectively, our study validates an effective EGFR-targeted chitosan carrier for siRNA, together with a promising therapeutic target, Mad2 and also shows that siRNA can be an effective strategy in cancer therapy by itself or in combination with anticancer drugs to increase the therapeutic potential of these drugs.

Supplementary Material

Refer to Web version on PubMed Central for supplementary material.

Acknowledgments

This study was supported by a grant from the National Cancer Institute's (NCI) Alliance for Nanotechnology in Cancer Platform Partnership (CNPP) grant U01-CA151452 and by NCI R21 grant CA179652-01A1. This work was partially supported by CESPU under the project 02-CQF-CICS-776 2011N. Ana Vanessa Nascimento thanks the Fundação Ciência e Tecnologia (FCT), Portugal, for her Ph.D. grant no. SFRH/BD/69271/2010.

References

1. Siegel RL, Miller KD, Jemal A. Cancer statistics, 2015. *CA Cancer J Clin.* 2015; 65(1):5–29. [PubMed: 25559415]
2. Torre LA, Bray F, Siegel RL, Ferlay J, Lortet-Tieulent J, Jemal A. Global cancer statistics, 2012. *CA Cancer J Clin.* 2015; 65(2):87–108. [PubMed: 25651787]

3. Du L, Morgensztern D. Chemotherapy for Advanced-Stage Non-Small Cell Lung Cancer. *Cancer J*. 2015; 21(5):366–370. [PubMed: 26389760]
4. Smit E, Moro-Sibilot D, de Castro Carpeño J, Lesniewski-Kmak K, Aerts J, Villatoro R, Kraaij K, Nacerddine K, Dyachkova Y, Smith KT. Cisplatin and carboplatin-based chemotherapy in the first-line treatment of non-small cell lung cancer: analysis from the European FRAME study. *Lung Cancer*. 2015
5. Dasari S, Tchounwou PB. Cisplatin in cancer therapy: molecular mechanisms of action. *Eur J Pharmacol*. 2014; 740:364–378. [PubMed: 25058905]
6. Silva P, Barbosa J, Nascimento AV, Faria J, Reis R, Bousbaa H. Monitoring the fidelity of mitotic chromosome segregation by the spindle assembly checkpoint. *Cell Proliferation*. 2011; 44(5):391–400. [PubMed: 21951282]
7. Barbosa J, Nascimento AV, Faria J, Silva P, Bousbaa H. The spindle assembly checkpoint: perspectives in tumorigenesis and cancer therapy. *Frontiers in Biology*. 2011; 6(2):147–155.
8. Mueller S, Schittenhelm M, Honecker F, Malenke E, Lauber K, Wesselborg S, Hartmann JT, Bokemeyer C, Mayer F. Cell-cycle progression and response of germ cell tumors to cisplatin in vitro. *Int J Oncol*. 2006; 29(2):471–479. [PubMed: 16820891]
9. Wang D, Lippard SJ. Cellular processing of platinum anticancer drugs. *Nat Rev Drug Discov*. 2005; 4(4):307–320. [PubMed: 15789122]
10. Lawrence KS, Chau T, Engebrecht J. DNA damage response and spindle assembly checkpoint function throughout the cell cycle to ensure genomic integrity. *PLoS Genet*. 2015; 11(4):e1005150. [PubMed: 25898113]
11. Galluzzi L, Vitale I, Michels J, Brenner C, Szabadkai G, Harel-Bellan A, Castedo M, Kroemer G. Systems biology of cisplatin resistance: past, present and future. *Cell Death Dis*. 2014; 5:e1257. [PubMed: 24874729]
12. More SS, Akil O, Ianculescu AG, Geier EG, Lustig LR, Giacomini KM. Role of the copper transporter, CTR1, in platinum-induced ototoxicity. *J Neurosci*. 2010; 30(28):9500–9509. [PubMed: 20631178]
13. Sancho-Martinez SM, Prieto-Garcia L, Prieto M, Lopez-Novoa JM, Lopez-Hernandez FJ. Subcellular targets of cisplatin cytotoxicity: an integrated view. *Pharmacol Ther*. 2012; 136(1):35–55. [PubMed: 22796517]
14. Gao Y, Shen JK, Milane L, Hornicek FJ, Amiji MM, Duan Z. Targeted cancer therapy; nanotechnology approaches for overcoming drug resistance. *Curr Med Chem*. 2015; 22(11):1335–1347. [PubMed: 25666804]
15. Amer MH. Gene therapy for cancer: present status and future perspective. *Mol Cell Ther*. 2014; 2:27. [PubMed: 26056594]
16. Mc Gee MM. Targeting the Mitotic Catastrophe Signaling Pathway in Cancer. *Mediators Inflamm*. 2015; 2015:146282. [PubMed: 26491220]
17. Choi M, Kim W, Cheon MG, Lee CW, Kim JE. Polo-like kinase 1 inhibitor BI2536 causes mitotic catastrophe following activation of the spindle assembly checkpoint in non-small cell lung cancer cells. *Cancer Lett*. 2015; 357(2):591–601. [PubMed: 25524551]
18. Silva P, Barbosa J, Nascimento AV, Faria J, Reis R, Bousbaa H. Monitoring the fidelity of mitotic chromosome segregation by the spindle assembly checkpoint. *Cell Prolif*. 2011; 44(5):391–400. [PubMed: 21951282]
19. Dotiwala F, Harrison JC, Jain S, Sugawara N, Haber JE. Mad2 prolongs DNA damage checkpoint arrest caused by a double-strand break via a centromere-dependent mechanism. *Curr Biol*. 2010; 20(4):328–332. [PubMed: 20096585]
20. Magiera MM, Gueydon E, Schwob E. DNA replication and spindle checkpoints cooperate during S phase to delay mitosis and preserve genome integrity. *J Cell Biol*. 2014; 204(2):165–175. [PubMed: 24421333]
21. Cheung HW, Jin DY, Ling MT, Wong YC, Wang Q, Tsao SW, Wang X. Mitotic arrest deficient 2 expression induces chemosensitization to a DNA-damaging agent, cisplatin, in nasopharyngeal carcinoma cells. *Cancer Res*. 2005; 65(4):1450–1458. [PubMed: 15735033]

22. Michel L, Diaz-Rodriguez E, Narayan G, Hernando E, Murty VV, Benezra R. Complete loss of the tumor suppressor MAD2 causes premature cyclin B degradation and mitotic failure in human somatic cells. *Proc Natl Acad Sci U S A*. 2004; 101(13):4459–4464. [PubMed: 15070740]
23. Nascimento AV, Singh A, Bousbaa H, Ferreira D, Sarmento B, Amiji MM. Mad2 checkpoint gene silencing using epidermal growth factor receptor-targeted chitosan nanoparticles in non-small cell lung cancer model. *Molecular pharmaceutics*. 2014; 11(10):3515–3527. [PubMed: 25256346]
24. Shi Q, Hu M, Luo M, Liu Q, Jiang F, Zhang Y, Wang S, Yan C, Weng Y. Reduced expression of Mad2 and Bub1 proteins is associated with spontaneous miscarriages. *Mol Hum Reprod*. 2011; 17(1):14–21. [PubMed: 20643875]
25. Castedo M, Perfettini JL, Roumier T, Andreau K, Medema R, Kroemer G. Cell death by mitotic catastrophe: a molecular definition. *Oncogene*. 2004; 23(16):2825–2837. [PubMed: 15077146]
26. Floor SL, Dumont JE, Maenhaut C, Raspe E. Hallmarks of cancer: of all cancer cells, all the time? *Trends Mol Med*. 2012; 18(9):509–515. [PubMed: 22795735]
27. Deng Y, Wang CC, Choy KW, Du Q, Chen J, Wang Q, Li L, Chung TK, Tang T. Therapeutic potentials of gene silencing by RNA interference: principles, challenges, and new strategies. *Gene*. 2014; 538(2):217–227. [PubMed: 24406620]
28. Miele E, Spinelli GP, Miele E, Di Fabrizio E, Ferretti E, Tomao S, Gulino A. Nanoparticle-based delivery of small interfering RNA: challenges for cancer therapy. *Int J Nanomedicine*. 2012; 7:3637–3657. [PubMed: 22915840]
29. Akhtar S, Benter IF. Nonviral delivery of synthetic siRNAs in vivo. *J Clin Invest*. 2007; 117(12):3623–3632. [PubMed: 18060020]
30. Kean T, Thanou M. Biodegradation, biodistribution and toxicity of chitosan. *Advanced drug delivery reviews*. 2010; 62(1):3–11. [PubMed: 19800377]
31. Liu X, Howard KA, Dong M, Andersen MO, Rahbek UL, Johnsen MG, Hansen OC, Besenbacher F, Kjems J. The influence of polymeric properties on chitosan/siRNA nanoparticle formulation and gene silencing. *Biomaterials*. 2007; 28(6):1280–1288. [PubMed: 17126901]
32. Rudzinski WE, Aminabhavi TM. Chitosan as a carrier for targeted delivery of small interfering RNA. *International journal of pharmaceutics*. 2010; 399(1):1–11. [PubMed: 20732398]
33. Nascimento AV, Singh A, Bousbaa H, Ferreira D, Sarmento B, Amiji MM. Combinatorial-Designed Epidermal Growth Factor Receptor-Targeted Chitosan Nanoparticles for Encapsulation and Delivery of Lipid-Modified Platinum Derivatives in Wild-Type and Resistant Non-Small-Cell Lung Cancer Cells. *Mol Pharm*. 2015
34. Andersen MO, Howard KA, Kjems J. RNAi using a chitosan/siRNA nanoparticle system: in vitro and in vivo applications. *Methods Mol Biol*. 2009; 555:77–86. [PubMed: 19495689]
35. Gref R, Lück M, Quellec P, Marchand M, Dellacherie E, Harnisch S, Blunk T, Müller R. ‘Stealth’ corona-core nanoparticles surface modified by polyethylene glycol (PEG): influences of the corona (PEG chain length and surface density) and of the core composition on phagocytic uptake and plasma protein adsorption. *Colloids and Surfaces B: Biointerfaces*. 2000; 18(3):301–313. [PubMed: 10915952]
36. Tiera MJ, Shi Q, Barbosa HF, Fernandes JC. Polymeric systems as nanodevices for siRNA delivery. *Curr Gene Ther*. 2013; 13(5):358–369. [PubMed: 24369060]
37. Nascimento AV, Gattacceca F, Singh A, Bousbaa H, Ferreira D, Sarmento B, Amiji MM. Biodistribution and pharmacokinetics of Mad2 siRNA-loaded EGFR-targeted chitosan nanoparticles in cisplatin sensitive and resistant lung cancer models. *Nanomedicine*. 2016; (0)
38. Howard KA, Rahbek UL, Liu X, Damgaard CK, Glud SZ, Andersen MO, Hovgaard MB, Schmitz A, Nyengaard JR, Besenbacher F, Kjems J. RNA interference in vitro and in vivo using a novel chitosan/siRNA nanoparticle system. *Molecular therapy : the journal of the American Society of Gene Therapy*. 2006; 14(4):476–484. [PubMed: 16829204]
39. Raja MA, Katas H, Jing Wen T. Stability, Intracellular Delivery, and Release of siRNA from Chitosan Nanoparticles Using Different Cross-Linkers. *PloS one*. 2015; 10(6):e0128963. [PubMed: 26068222]
40. O’Grady S, Finn SP, Cuffe S, Richard DJ, O’Byrne KJ, Barr MP. The role of DNA repair pathways in cisplatin resistant lung cancer. *Cancer treatment reviews*. 2014; 40(10):1161–1170. [PubMed: 25458603]

41. Galluzzi L, Senovilla L, Vitale I, Michels J, Martins I, Kepp O, Castedo M, Kroemer G. Molecular mechanisms of cisplatin resistance. *Oncogene*. 2012; 31(15):1869–1883. [PubMed: 21892204]
42. Tao W. The mitotic checkpoint in cancer therapy. *Cell Cycle*. 2005; 4(11):1495–1499. [PubMed: 16258280]

Author Manuscript

Author Manuscript

Author Manuscript

Author Manuscript

Statement of Significance

Lung cancer remains one of the leading killers in the United States and around the world. Platinum agents, including cisplatin, are the first line treatment in lung cancer, including non-small cell lung cancer (NSCLC), which is the predominant form of lung cancer. In this study, we have evaluated *Mad2* cell-cycle checkpoint gene silencing using small interfering RNA (siRNA) delivered systemically using epidermal growth factor receptor-targeted chitosan nanoparticles in drug sensitive and resistant models of NSCLC. Our results for the first time show that *Mad2* gene silencing using targeted chitosan nanoparticles has tremendous potential in overcoming platinum resistance in NSCLC.

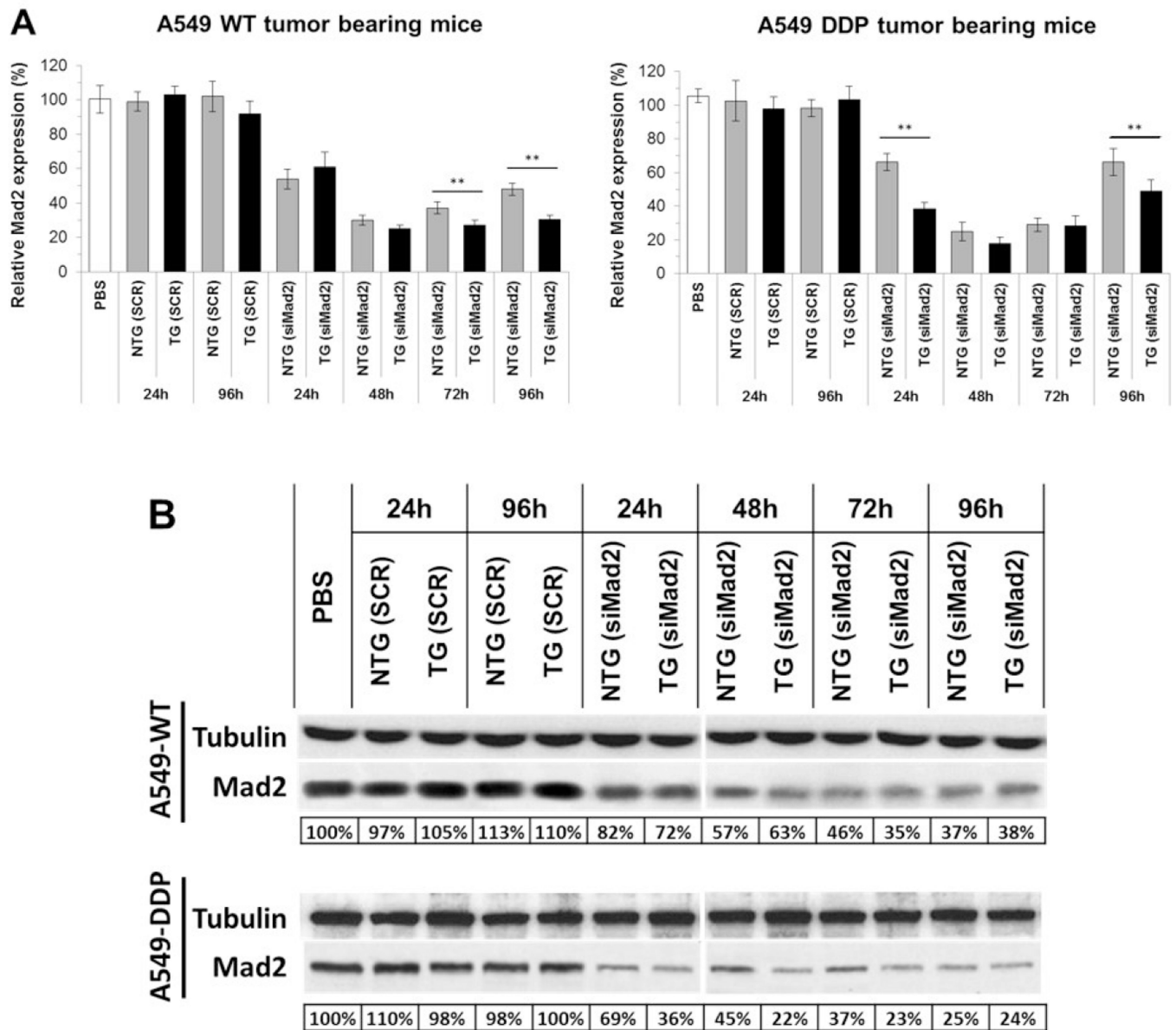


Figure 1. Knockdown efficiency of siRNA targeting Mad2 in NSCLC tumor bearing mice
 (A) qPCR and (B) western blot analysis of Mad2 knockdown efficiency in A549 WT and A549 DDP tumors. A 3 mg/kg single dose of siRNA, encapsulated either in TG or NTG NPS, was administered to tumor bearing mice. Tumors were collected at different time points for evaluation of the Mad2 gene silencing. (n = 5 animals/group). On qPCR data, bars represent the mean \pm standard deviation from three independent experiments. *** = $p < 0.01$. Referring to the western data, tubulin protein was used as an internal control. Below each set of western blot are the values of the relative density of Mad2 protein levels, which were normalized to those of tubulin. Data represents one of the three independent experiments with similar results. DDP: Cisplatin; NTG: Non Targeted; SCR, scramble sequence siRNA; SD: Standard Deviation; TG: Targeted; WT: Wild Type

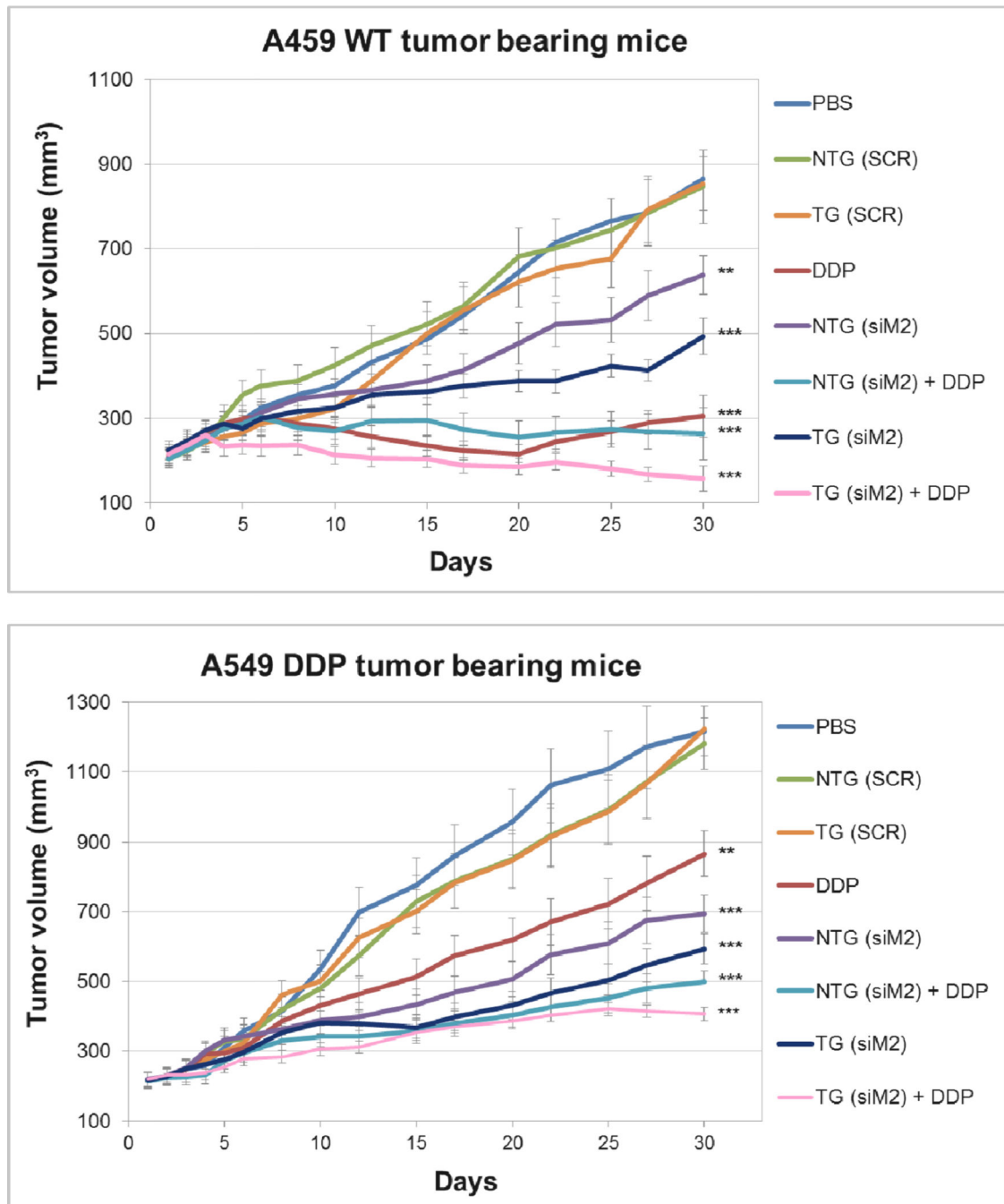


Figure 2. Effect of the combination of cisplatin treatment and Mad2 silencing on growth of sensitive and resistant A549 tumor bearing mice

Tumor volume variations for the different treatments intravenously injected in A549 WT and A549 DDP tumor bearing mice. $n = 8$ mice. ** $p < 0.01$, *** $p < 0.001$ (t-test comparing to PBS treatment).

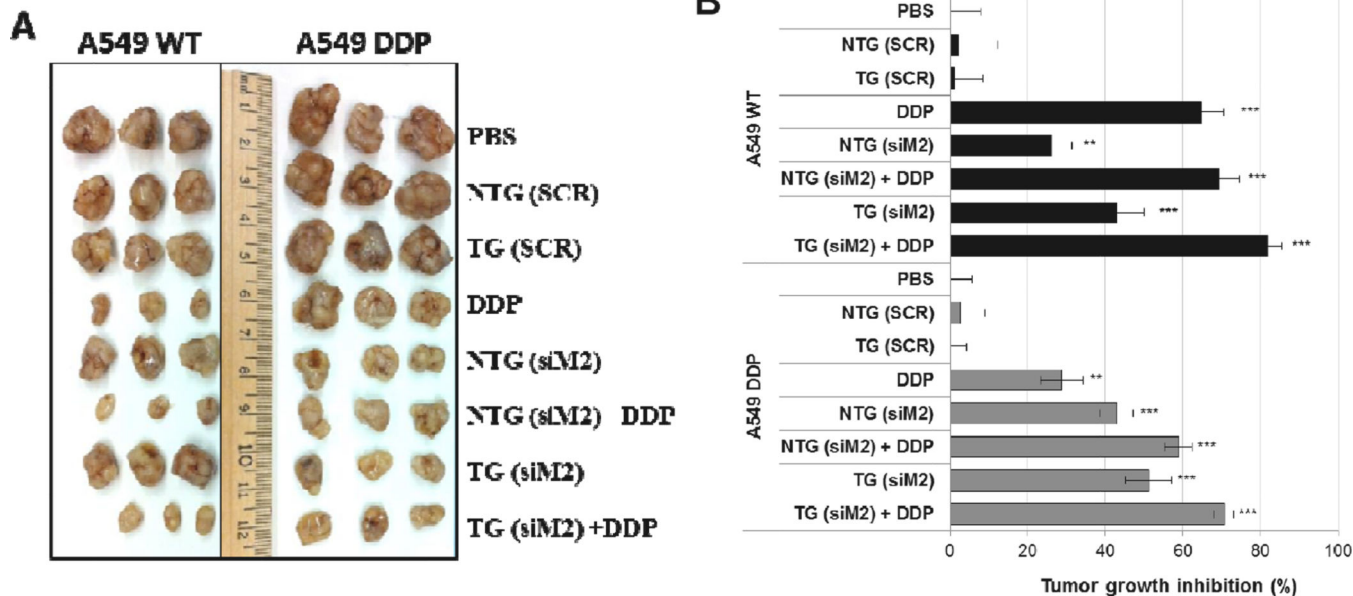
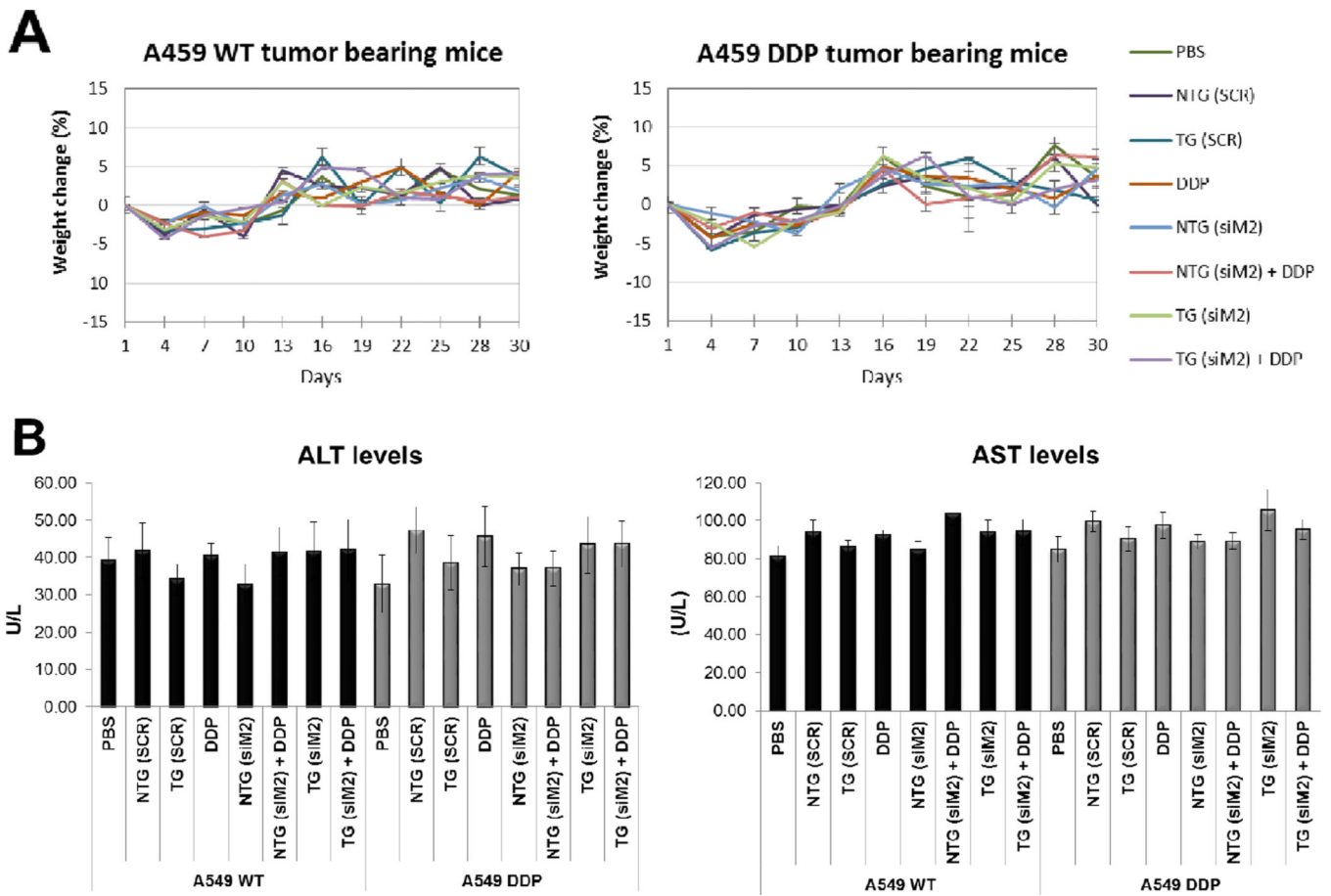


Figure 3. A549 WT and A549 DDP xenograft tumors (A) and percentage tumor growth inhibition following treatment with single or combination therapy of Mad2 siRNA and cisplatin in sensitive and resistant A549 tumor bearing mice
 n = 8 mice, ** p<0.01, *** p<0.001 (t-test comparing to PBS treatment).



Author Manuscript

Author Manuscript

Author Manuscript

Author Manuscript

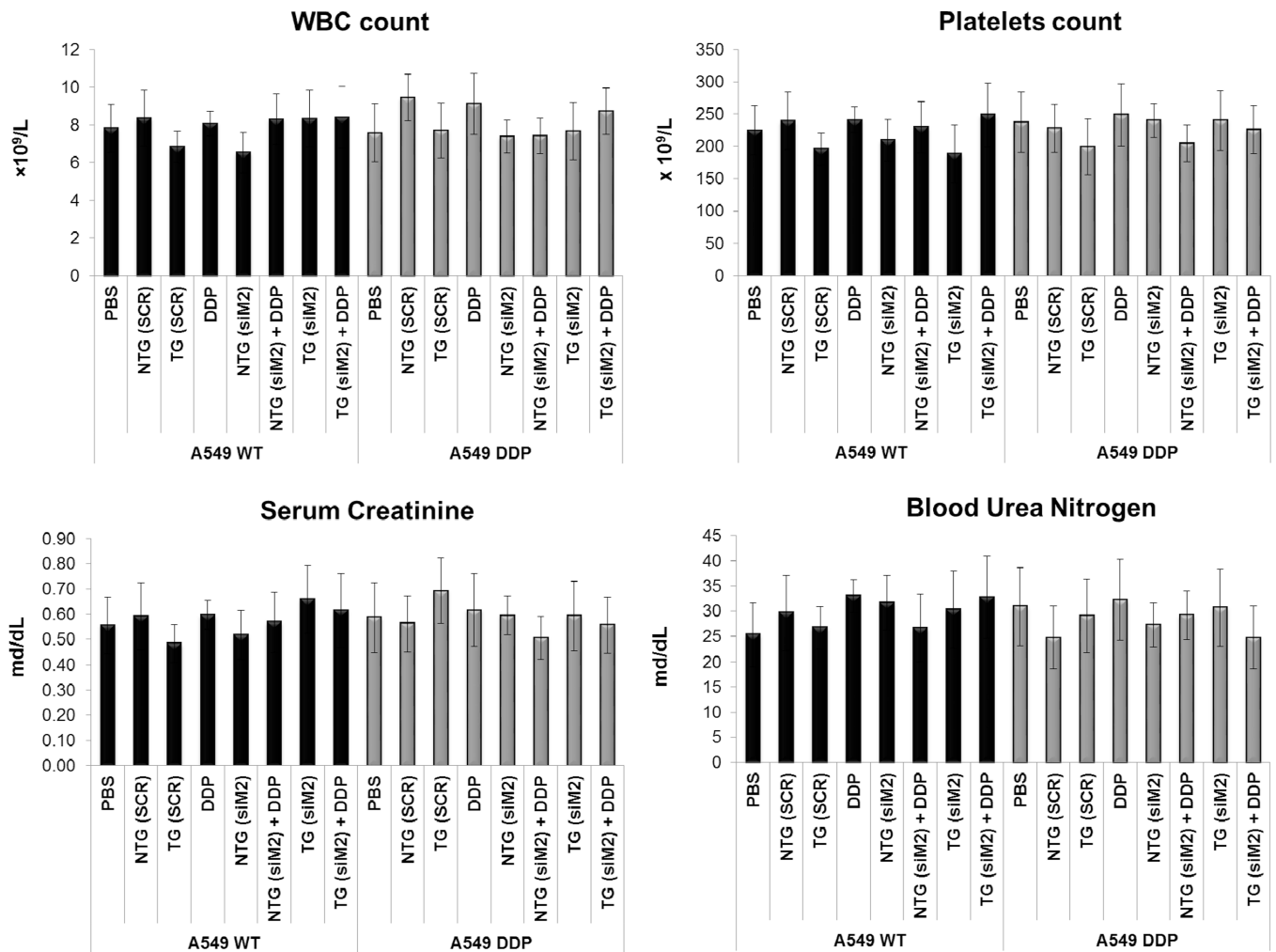


Figure 4. Safety profile

(A) Body weight variations mice from different treatment of A549 WT and A549 DDP tumor bearing mice. (B) Histograms that show the levels of several safety parameters in the different treatment groups. The parameters tested were: the concentrations of the enzymes aspartate transaminase (AST) and alanine transaminase (ALT) that are reasonably sensitive indicators of liver damage; the number of white blood cells (WBC); the number of platelets; serum creatinine and blood urea nitrogen as indicators of kidney function.

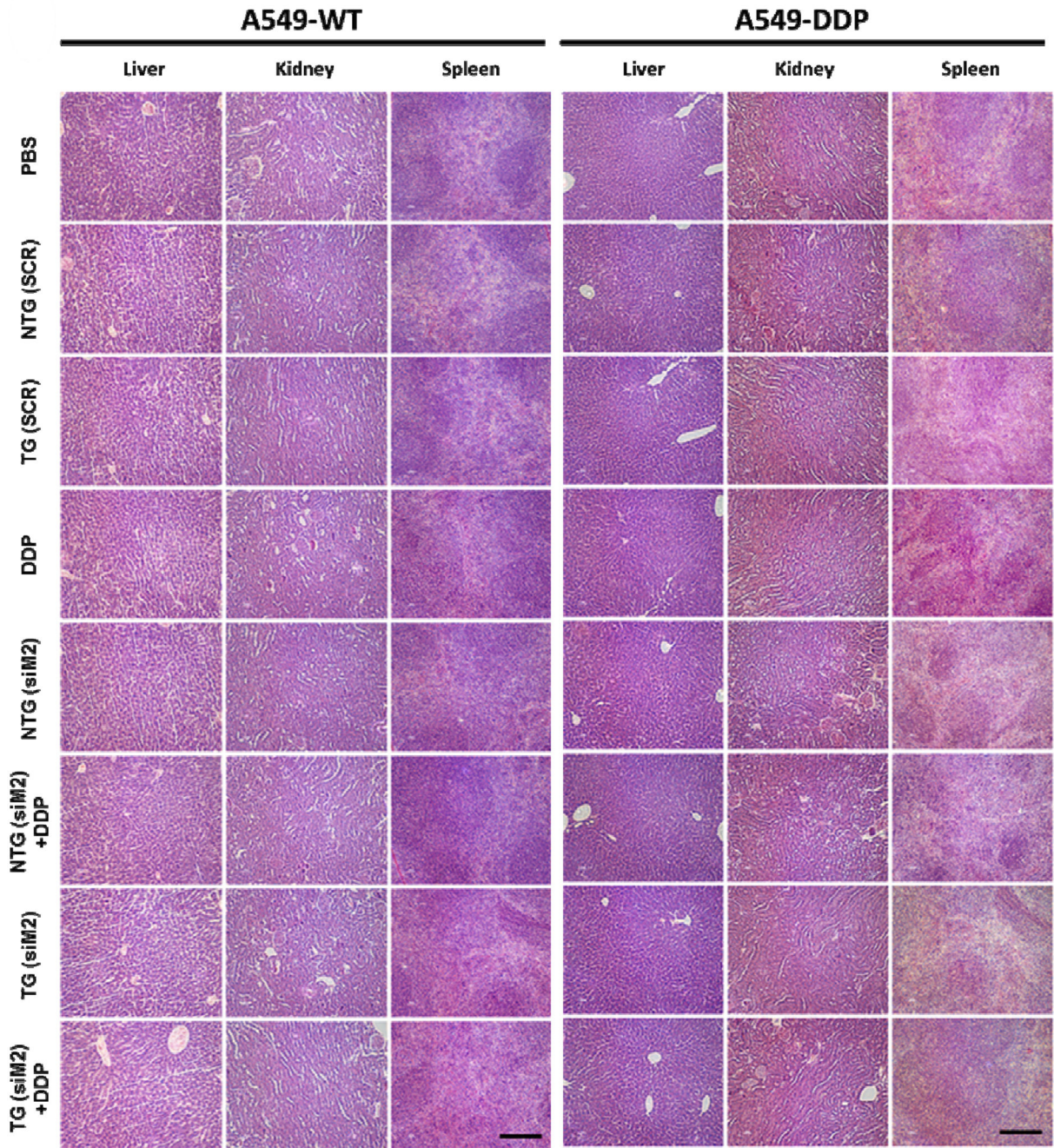


Figure 5. Histological sections after H&E staining of liver, kidney, and spleen from mice from different treatment of (A) A549 WT and (B) A549 DDP tumor bearing mice
Scale bar = 100 μ m.

Author Manuscript

Author Manuscript

Author Manuscript

Author Manuscript

CS nanoparticles characterization (particle size, zeta-potential, and siMad2 encapsulation efficiency) of CS/siRNA nanoparticles at a NP ratio of 50.

Table 1

NTG	126.7 ± 3.7	0.421 ± 0.072	+27.8 ± 3.5	95.5 ± 2.3	3.6 ± 0.73
TG	202.7 ± 2.5	0.316 ± 0.027	+21.2 ± 2.4	96.4 ± 7.5	4.82 ± 0.39

Table 2

IC₅₀ values of free cisplatin treatment, 48h post-transfection with siMad2 encapsulated in TG or NTG NPs in A549-WT (A) and A549-DDP (B) cells.

A549-WT	DDP	12.24 ± 1.09	—
	Lipofectamine (siMad2 50 nM)	0.306 ± 0.008	40× less
	NTG (siMad2 50 nM)	0.999 ± 0.015	12× less
	TG (siMad2 50 nM)	0.132 ± 0.012	95× less
A549-DDP	DDP	142.204 ± 2.156	—
	Lipofectamine (siMad2 5nM)	0.325 ± 0.017	437× less
	NTG (siMad2 1 nM)	0.178 ± 0.021	799× less
	TG (siMad2 1 nM)	0.094 ± 0.023	1513× less
	NTG (siMad2 5 nM)	0.086 ± 0.033	1653× less
	TG (siMad2 5 nM)	0.057 ± 0.031	2495× less